

# Frequency band tunable antenna with parasitic element to switch between narrow band and notched UWB for Personal Area Network Applications

M. Nirmala<sup>1</sup> and N. Deepika Rani<sup>2</sup>

<sup>1</sup>Department of ECE, Anil Neerukonda Institute of Technology and Sciences (Autonomous), Visakhapatnam-531162, Andhra Pradesh, India

<sup>2</sup>Department of ECE, Gayatri Vidya Parishad College of Engineering (Autonomous), Visakhapatnam-530048, Andhra Pradesh, India

Corresponding author: M.Nirmala (e-mail: nirmala.mattaparathi@gmail.com).

**ABSTRACT** This paper presents a compact frequency-band tunable antenna (FBTA) capable of reconfiguring its operation between a notched ultra-wideband (UWB) mode and a narrowband mode using a single radiating element. The proposed monopole antenna incorporates a strip line feed and a non-uniform ground structure to achieve a wide impedance bandwidth from 3.6 GHz to 10.85 GHz. Frequency-band configurability is enabled through the integration of an open-ended triangular parasitic element and PIN diodes within the ground plane, eliminating the need for radiator modification. In the notched UWB configuration, the antenna exhibits effective band-rejection characteristics from 5.06 GHz to 5.93 GHz, thereby suppressing interference from Wireless Local Area Network (WLAN) systems in compliance with FCC regulations. By varying the biasing states of the PIN diodes, the antenna dynamically switches between notched UWB and narrowband responses. The antenna is realized on a compact 40 mm × 30 mm × 1.6 mm FR4 substrate, and its impedance bandwidth and radiation characteristics are evaluated under different switching conditions. The proposed design offers a simple and efficient solution for reconfigurable wireless applications requiring compact size and flexible frequency operation.

**INDEX TERMS** Frequency-Band Tunable Antenna (FBTA), Frequency Configurability, Notch band, PIN Diodes, Ultra-wideband

## I. INTRODUCTION

The frequency range that the FCC [1] authorized for Ultra Wide Band (UWB) applications ranges from 3.1 GHz to 10.6 GHz. UWB transmissions utilize a fractional frequency bandwidth of more than 20%, or 500 MHz, for their spectral occupancy. This frequency range allows precise location tracking with high-speed information transmission. UWB technology has gained popularity in various industries, including healthcare, automotive, and telecommunications, due to its ability to transmit large amounts of data with low power consumption. UWB has become more widely recognized as one of the most promising wireless technologies because of high speed data transmission rate. The Unlicensed Personal Area Networks (UPANs) allow wireless communication between personal devices without requiring a particular regulatory authorization. The advantage of UPAN technologies is that they are accessible and simple to use. Personal Area Networks for local access are cheaper. The UWB spectrum is utilized by unlicensed narrow-band services that include IEEE 802.11a WLAN (5.15GHz–5.35GHz, 5.725GHz–5.825GHz) and Wi-Max (5.8GHz). These unlicensed wireless services may interfere with other

services in the UWB frequency spectrum. FCC specifies Equivalent Isotropic Radiated Power (EIRP) for 3.1GHz – 10.6GHz band as maximum -41.3dBm [1]. Ultra wideband (UWB) antennas are widely used in communication systems because of their smaller profile, cost-effectiveness, light-weight, simple design, easy manufacture, wider impedance bandwidth, and wide variety of compatibility with different microstrip circuits. A monopole antenna [2] operates in a spectrum from 1.3 GHz to 3 GHz for improved gain. Researchers have also employed a range of methods, such as tapered-shaped defective ground structures and rectangular slots, to attain ultra-wide bandwidth. A variety of design solutions are used to increase microstrip antennas' gain and bandwidth, including modified ground planes (MGPs) and microstructures such as Split-Ring Resonators (SRRs), Electromagnetic Band Gaps (EBGs), and parasitic element loading. Parasitic element design involves fractal structures. UWB antennas have been suggested for achieving band-notch properties [3-4]. By adopting a unique feeding mechanism, twin slits are taken within the elliptically shaped radiating element to provide dual-band notch features [5]. According to research findings, numerous techniques are employed to obtain

notch band characteristics in the UWB frequency range. Some of these techniques include placing parasitic elements on the ground plane, folded strips on the truncated ground plane, a radiating patch with tapered line resonator, etching bend slits on radiators, and the ground plane with open-circuiting stubs to achieve notch band response in the desired frequency range [6-10]. In order to maintain a reliable and efficient communication system and avoid interference, it is necessary to switch between multiple frequency bands. Implementing band notching in UWB antennas is one method of reducing interference. In order to achieve the band notching, the reported antennas commonly employ a half-wavelength slot design in the shape of U, C, and arched [11-13]. There is extensive discussion of several methods for achieving single and multiple notched-band functions in [14-18]. Reshaping a radiating element and adding several slots to a patch enables the antenna's performance to resonate in a wide band [19-20]. A frequency reconfigurable antenna with complementary characteristics is obtained by using an F-shaped parasitic element, a pair of SRRs, and PIN diodes [21-22].

In this work, a Frequency Band Tunable Antenna (FBTA), which switches its operating frequency band characteristics from a notched ultra-wideband to a narrow band, is developed. A monopole antenna is designed with strip line feed and a non-uniform ground structure. The ground is designed to widen the impedance band from 3.6 GHz to 10.85 GHz to achieve ultra-wideband. The antenna's characteristics can be switched from notched UWB to narrow band by changing the PIN diodes' biasing conditions positioned in the patch's ground plane, which makes complementary frequency band configurability possible.

## II. ANTENNA DESIGN PROCEDURE

### A. Monopole Antenna

A monopole antenna is designed and modified to obtain the UWB frequency response. Using (1-3) [23] as shown in Fig.1(a), a circular monopole antenna with a patch radius (R) of 10.5 mm has been designed to operate at 7.59 GHz on a rectangular substrate of 30 mm × 40 mm × 1.6 mm. The substrate material is FR4 glass epoxy with a dielectric constant ( $\epsilon_r$ ) of 4.4, a loss tangent ( $\delta$ ) of 0.02, and a dielectric thickness of 1.6 mm. A 50  $\Omega$  microstrip line of length ( $L_f$ ) 13.575 mm is used for feeding. Using (4-6) [23], the feed line width  $L_w$  is calculated to be 2.5 mm.

$$f_r = \frac{1.8412 \times c}{2\pi \times a \times \sqrt{\epsilon_{eff}}} \quad (1)$$

$$\epsilon_{eff} = \frac{\epsilon_r + 1}{2} \quad (2)$$

$$a = R \times \sqrt{1 + \frac{4H}{2\pi \times r \times \epsilon_r} \left[ \ln \left( \frac{2\pi \times r}{4H} \right) + 1.77 \right]} \quad (3)$$

Where

c= Velocity of EM wave in air 3 x 10<sup>8</sup> m/s

a= circular monopole effective radius,

R= circular monopole actual radius and  
H= Substrate thickness.

$$\frac{L_w}{H} = \begin{cases} \frac{8e^A}{e^{2A}-2}, & \frac{L_w}{H} \leq 2 \\ \frac{2}{\pi} \left\{ B - 1 - \ln(2B - 1) + \frac{\epsilon_r - 1}{2\epsilon_r} \left[ \ln(B - 1) + 0.39 - \frac{0.61}{\epsilon_r} \right] \right\}, & \frac{L_w}{H} \geq 2 \end{cases} \quad (4)$$

$$A = \frac{2\pi Z_0}{\eta} \sqrt{\frac{\epsilon_r + 1}{2}} + \frac{\epsilon_r - 1}{\epsilon_r + 1} \left( 0.23 + \frac{0.11}{\epsilon_r} \right) \quad (5)$$

$$B = \frac{\eta}{2Z_0 \sqrt{\epsilon_r}} \quad (6)$$

Normal ground located on the back plane of the circular patch has dimensions of L = 40 mm and W = 30 mm as presented in Fig.1(a). The monopole antenna operates at 7.59 GHz.

### B. UWB Antenna Design

Antenna's operating bandwidth can be improved by using defected ground structures and modified ground planes. By using these methods, the antenna's efficiency is increased, and reflections are minimized. The ground width (W) = 30mm is the same as the substrate width, and the ground length  $L_g$  of 13.09 mm has been modified to enhance bandwidth. As seen in Fig.1(b), the outside border of the metallic ground plane is modified by using a rectangular slit with dimensions of 4 mm × 1 mm. The rectangular slit helps to improve the performance of the metallic ground plane.

It has been noticed that the length of the current path on the surfaces of the ground outside the border is improved by doubling the slot length (SI). In the case of an unmodified ground plane, the length of the current path at the outside edge is W = 30 mm; however, when a rectangular slot is present on the top edge, it becomes W + 2 × SI = 32 mm. The rectangular-shaped slot on the upper portion of the Modified Ground Plane (MGP) changes the surface current distribution, which provides additional resonance frequencies in the lower and upper ranges. These additional resonance frequencies can enhance the performance of antennas operating in those frequency bands. The presence of the rectangular slot alters the electromagnetic field distribution, resulting in improved radiation characteristics and increased bandwidth for the MGP. A modified circular patch is designed for further improvement in UWB resonance. Reshaping of the circular patch structure by cutting semicircular sections on both edges, as represented in Fig.1(c), leads to better impedance bandwidth in the UWB range. In comparison with the antenna without MGP and patch structure modifications, the designed monopole UWB antenna with modified ground and patch structure has an extended impedance bandwidth. The physical dimensions of the designed monopole UWB antenna presented in Fig.1 are: Length of the ground ( $L_g$ ) = 13.09 mm, Feed line length ( $L_f$ ) = 13.575 mm, Feed line width ( $L_w$ ) = 2.5 mm, Circular patch radius (R) = 10.5 mm, semicircular cut radius ( $r_1$ ) = 5 mm, Width of the ground slot ( $S_w$ ) = 4 mm, Length of the ground slot (SI) = 1 mm and  $L_c$  = 13.97 mm.

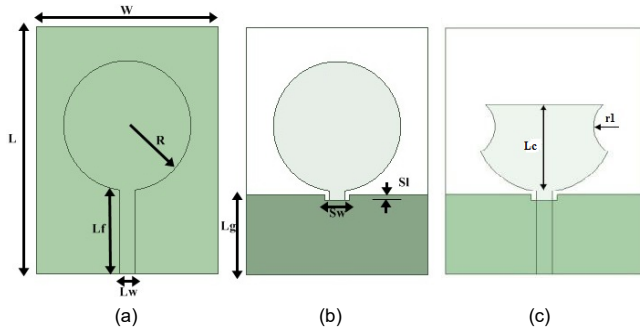


FIGURE 1. UWB Monopole antenna iterations, (a) Antenna 1, (b) Antenna 2, (c) UWB Antenna

From Fig.2, Antenna 1 exhibits the resonance at 7.59 GHz frequency. In order to extend the bandwidth of Antenna 1, the ground plane is modified. This helps to reduce the effects of ground losses and improves the antenna's overall performance, which makes Antenna 2 exhibit an impedance bandwidth of 8.65 GHz (from 3.03 GHz to 11.68 GHz). From 6.5 GHz to 7.2 GHz, the reflection coefficient  $S_{11}$ (dB) is very close to -10 dB. The UWB antenna has improved impedance bandwidth over UWB resonance by cutting semicircular sections on both edges of the circular patch. The UWB monopole antenna has a wider bandwidth of 8.41 GHz (from 3.04 GHz to 11.45 GHz).

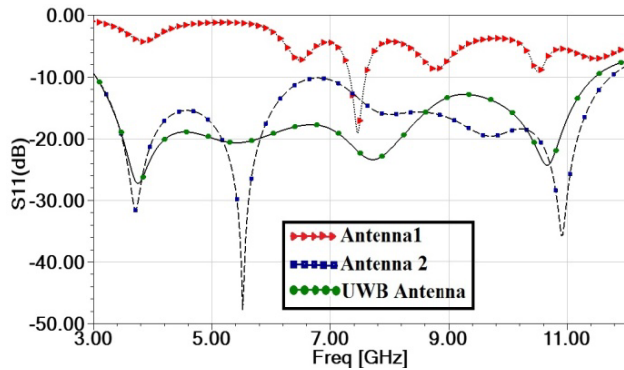


FIGURE 2. Reflection Coefficient for UWB Antenna iterations

### III.FREQUENCY BAND TUNABLE ANTENNA (FBTA)

To overcome the interference for WLAN applications, FBTA is proposed, designed, and implemented using an experimental setup. A band notch is obtained by loading the antenna with an open-ended triangular parasitic element and PIN diodes embedded on the ground plane. The guided wavelength ( $\lambda_g$ ) of an open-ended triangular-shaped parasitic element at 5.5 GHz is calculated using (7).

$$\lambda_g = \frac{c}{f_0 \sqrt{\epsilon_{eff}}} \quad (7)$$

An equilateral triangle is designed with arm outer length  $L_t = 12.09$  mm and arm width  $W_t = 0.5$  mm. The base side of the arm is opened with a gap distance of  $G = 0.6$  mm. The back plane view of the designed frequency band reconfigurable monopole antenna is represented in Fig.3(a).

The current distribution on a patch antenna surface is influenced by the condition of any integrated diodes, which can significantly impact the functionality of the antenna. Diodes can alter the antenna's resonance frequency, radiation pattern, and overall performance depending on whether they are in forward bias or reverse bias. The current distribution on the antenna surface is influenced by the geometry of the antenna, the operating frequency, and the specific characteristics of the integrated diodes. Two BAR 64-02VH6327 (SC79) RF PIN Diodes are placed between the ground plane and open-ended triangular parasitic element as illustrated in Fig.3(b).

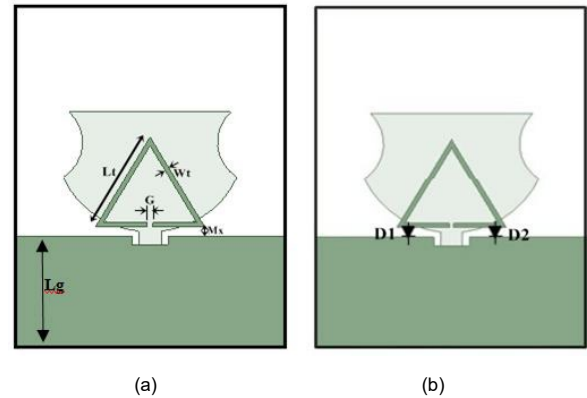


FIGURE 3. Designed Antenna Ground Plane (a) without PIN Diodes and (b) with PIN Diodes

### IV.PARAMETRIC ANALYSIS AND RESULTS

The return loss characteristics (negative of reflection coefficient in dB) of the designed antenna are observed with the effective variation of position ( $M_x$ ) parameter (the distance between the top edge of the ground plane and the base of the triangular element) at  $L_g = 13.09$  mm. When an open-ended triangular parasitic element is nearer to the ground top edge at a distance of 1.6 mm, band rejection characteristics are from 5.2 GHz to 5.8 GHz with a return loss of 3 dB. If  $M_x = 2$  mm and 2.4 mm, the rejection bandwidth gets narrower (from 5.3 GHz to 5.6 GHz, with a bandwidth of 0.3 GHz). The optimum position is considered at  $M_x = 1.6$  mm with respect to ground position ( $L_g$ ). The simulated parametric results are presented in Fig.4.

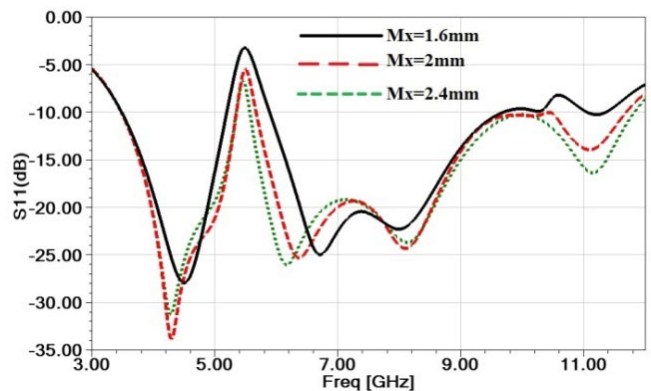


FIGURE 4. Reflection coefficient of Monopole UWB by varying the position of the parasitic element

The distance variation is created virtually by using two PIN diodes as shown in Fig.3(b). The PIN diodes exhibit  $2.1 \Omega$  resistances when in forward biased condition and  $3K \Omega$  resistances in parallel with  $0.17p$  F capacitance in reverse biased condition. The package inductance is the same for both biasing conditions, and its value is  $0.6n$  H. Fig.5 shows the antenna performance in two modes. Only two extreme modes of operating conditions, viz. ON-ON and OFF-OFF for diodes are considered. Fig.5 depicts that when two diodes D1 and D2 are in the OFF condition, the FBTA operates in Notched UWB mode. The return loss ( $S_{11}(dB)$ ) is below  $-10$  dB from  $3.58$  GHz to  $11.06$  GHz with a notch band from  $5.05$  GHz to  $5.93$  GHz. When two diodes D1 and D2 are in the ON condition, the FBTA operates in narrow-band mode. The return loss ( $S_{11}(dB)$ ) is below  $-10$  dB from  $5.12$  GHz to  $5.66$  GHz, narrow band. Complementary Frequency Band Reconfigurable characteristics are observed when the PIN diodes' biasing condition transition occurs. The proposed FBTA exhibits a significant frequency complementary reconfigurable property at WLAN applications ( $5.15$  GHz– $5.35$  GHz,  $5.725$  GHz– $5.825$  GHz) in two different operating modes.

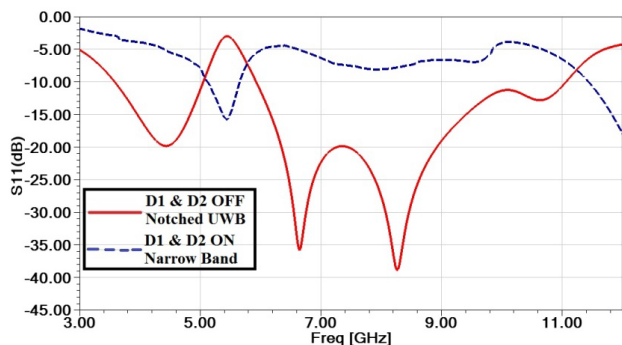


FIGURE 5. Simulated Return Loss of antenna at two extreme diode modes

The surface current distributions of the modified ground plane with different diode conditions are represented in Fig.6. As demonstrated in Figs. 6(a)–(c), when the diodes D1 and D2 are in the OFF state or reverse biased, the radiating frequencies are  $4.5$  GHz,  $5.5$  GHz, and  $6.7$  GHz, respectively. It is noted that the surface current distribution in the open-ended triangular parasitic element is more near at  $5.5$  GHz notch band, as presented in Fig.6(b). When D1 & D2 are in the ON state or forward biased, the surface currents presented on the ground plane and the open-ended triangular parasitic element edge are shown in Figs. 6(d)–(f) at  $4.5$  GHz,  $5.5$  GHz &  $6.7$  GHz, respectively.

The field patterns in the E and H-planes are observed in both states, i.e., when D1 & D2 are in OFF (reverse bias) and ON (forward bias) conditions at  $4.5$  GHz,  $5.5$  GHz, and  $6.7$  GHz. The design of effective wireless communication systems requires a thorough understanding of how the antenna interacts with its surroundings and radiates energy over a broad range of operating frequencies.

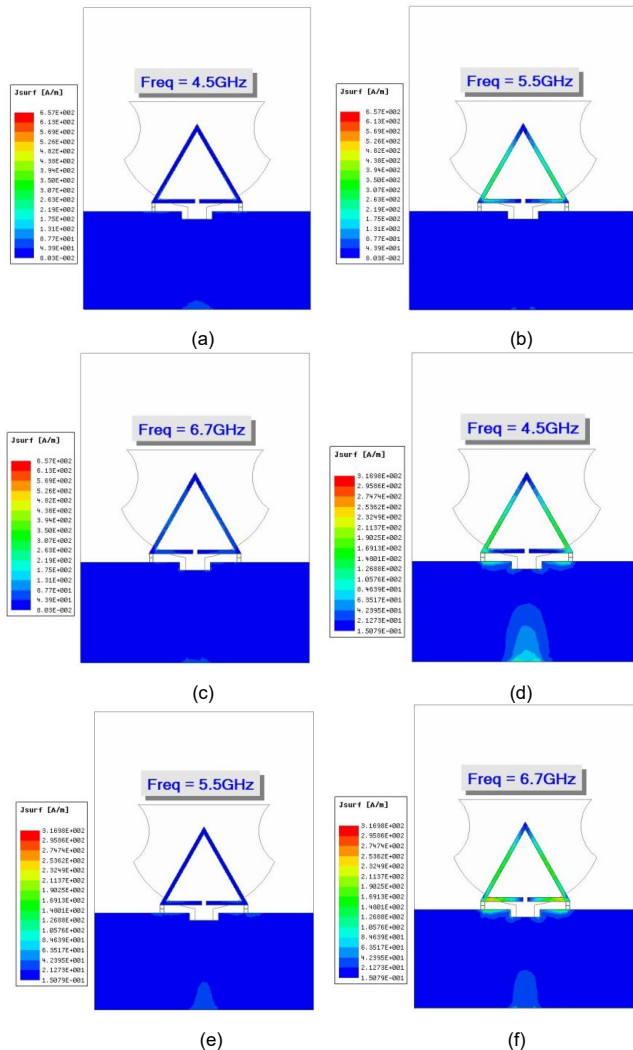
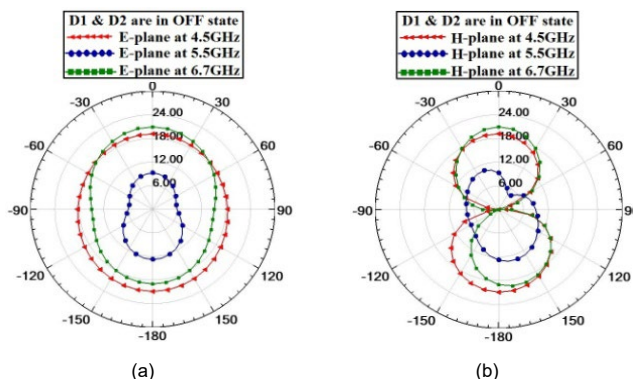


FIGURE 6. Surface currents D1 & D2 in OFF condition (a)-(c) and D1 & D2 in ON condition (d)-(f).

From Fig.7(a) & (b), it is depicted that the E-plane & H-plane are high and bidirectional at  $4.5$  GHz and  $6.7$  GHz, but at  $5.5$  GHz (notched band frequency), the radiation is very low. From Fig.7(c) & (d), it is observed that the E-plane and H-planes exhibit high radiation and bidirectional at a narrow band frequency of  $5.5$  GHz. The radiation is very low at frequencies  $4.5$  GHz and  $6.7$  GHz.



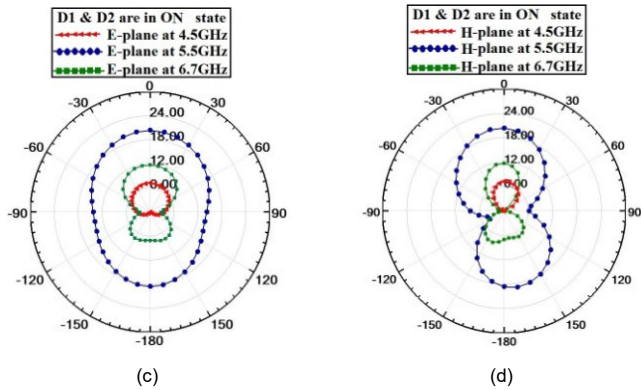


FIGURE 7. Measured Radiation patterns when FBTA in Notched UWB mode (a) E-plane (b) H-plane, and when FBTA in Narrow band mode (c) E-plane (d) H-plane

## V. RESULTS AND DISCUSSIONS

An FR4 substrate having a dielectric constant ( $\epsilon_r$ ) of 4.4 and a loss tangent ( $\delta$ ) of 0.02 with a 1.6 mm thickness is utilized for constructing the proposed Frequency Band Tunable Antenna. For signal transmission, a 50  $\Omega$  SMA connection is used. As seen in Fig.8, the constructed prototype antenna is tested and measured. The fabricated antenna performance is shown in Fig.9 when both diodes are in ON and OFF conditions.

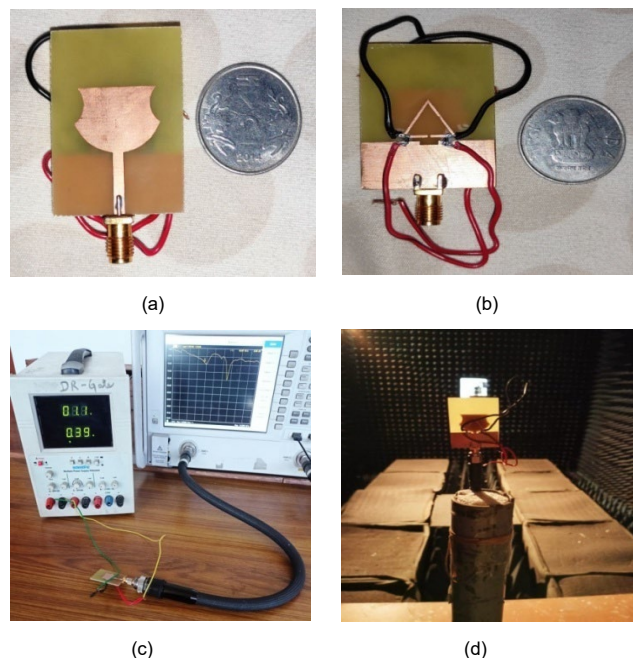


FIGURE 8. Prototype FBTA a) Top View, b) Bottom View, c) Experimental Setup, d) In Anechoic Chamber

As shown in Fig.9(a), band-notched characteristics (from 5.16 GHz to 5.97 GHz) have been observed in the resonant characteristics of FBTA. As shown in Fig.9(b), the FBTA resonant characteristics can be seen in a narrow band mode from 5.10 GHz to 5.65 GHz. In two different functioning modes, proposed FBTA exhibits considerable frequency complementary reconfigurable properties for WLAN applications (5.15 GHz–5.35 GHz and 5.725 GHz–

5.825 GHz). The properties of the designed antenna are within their limits.

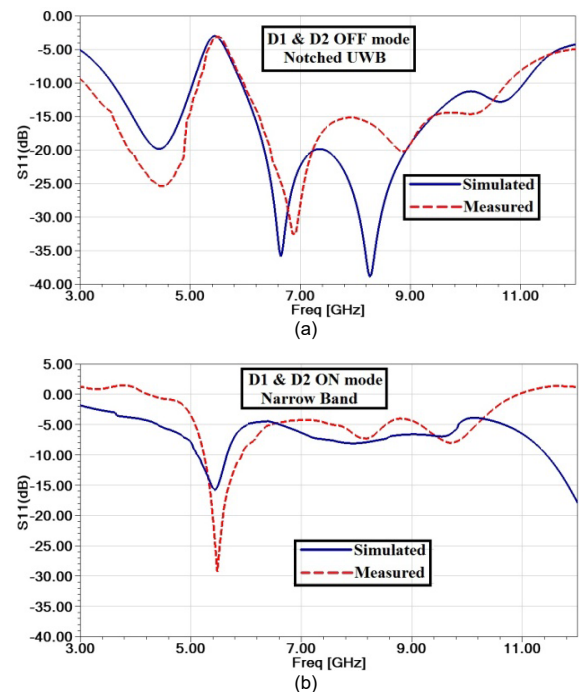
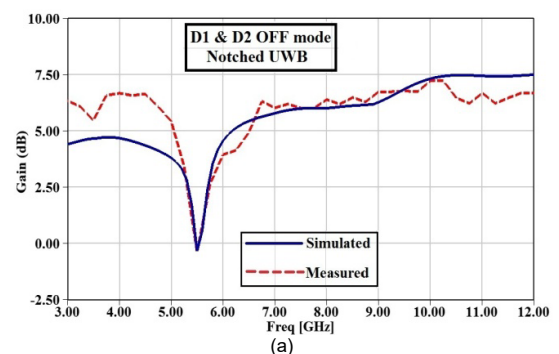


FIGURE 9. Simulated and Measured Return Loss of FBTA, (a) Notched UWB mode, (b) Narrow band mode

Fig.10 shows a comparison of both the simulated and tested results of the FBTA in two different operating modes. The radiation parameters of FBTA are complementary in nature at two different operating modes. As shown in Fig.10(a), when the diodes D1 & D2 are in the OFF condition (Notched UWB mode), in the notched frequency band from 5.2 GHz to 5.8 GHz, the gain of the designed FBTA is -1 dB. As it is expected in a notched UWB, the obtained gain is below 0 dB. When the diodes D1 & D2 are in ON condition (Narrow Band mode), the designed FBTA exhibits acceptable gain only at 5.5 GHz frequency. The gain is approximately 3.5 dB at 5.5 GHz frequency as shown in Fig.10(b). Antenna efficiency is measured in both the conditions of the diodes D1 & D2 and represented in Fig.10(c). Antenna efficiency is decreased to 20% at the notched frequency of 5.5 GHz in the Notched UWB mode. When in Narrow Band mode, an efficiency maximum of 73% is obtained at 5.5 GHz.



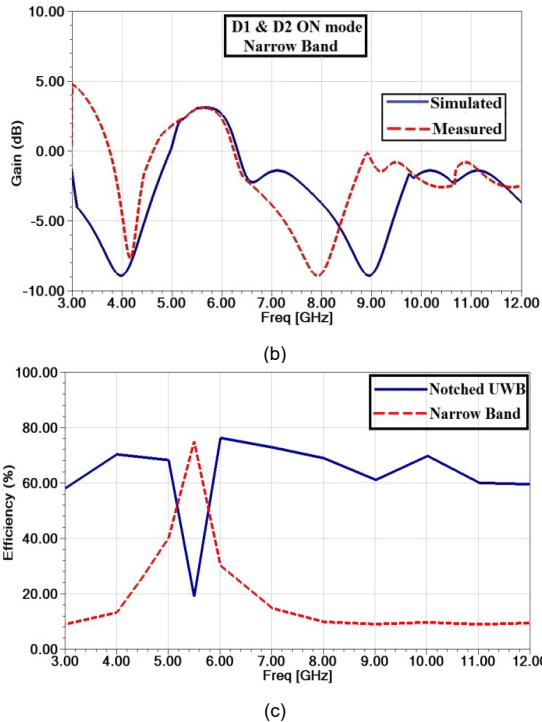


FIGURE 10. Comparison of simulated and measured (a) Gain in Notched UWB mode, (b) Gain in Narrow Band Mode, (c) Radiation Efficiency in two operating modes.

The minor variations are primarily due to practical fabrication tolerances, fluctuations in substrate dielectric characteristics, soldering and connector losses, and negligible losses in the measurement equipment, which are not entirely considered in the ideal simulation environment. Furthermore, environmental variables and mutual coupling effects during measurement may potentially account for these variations. In conclusion, despite the identified limitations, a clear consistency between simulation and measurement is maintained, demonstrating the reliability and efficacy of the proposed design.

TABLE 1. A comparative table

Feature	Ref. [3]	Ref. [6]	Ref. [22]	Proposed FBTA
Reconfiguration Type	Tunable band pass filter with varactor Diodes	Passive notch via parasitic elements	Electrical switching between notched and narrowband modes	PIN diode-controlled switching between notched UWB and narrowband
Switching Elements	4 Varactor Diodes	None	2 PIN Diodes + 2 SRRs	2 PIN Diodes
Structure Type	Wideband monopole + DGS filter	Monopole with two parasitic patches	CPW-fed monopole with embedded SRRs	Planar monopole with PIN diode switching stubs
Tuning Mechanism	Capacitance control in DGS	Geometry-dependent parasitic effect	PIN diode biasing to toggle between modes	PIN diode ON/OFF toggling for complementary behavior
Operating Modes	Tunable BPF response	Fixed Notched Band	Notched UWB ↔ Narrowband	Notched UWB ↔ Narrowband (complementary)

Operating Band	1.3GHz to 3GHz tuning range	3-10.1 GHz with notch at 5.15-5.825GHz	2.5-11 GHz UWB with notch at 6.01 GHz; Narrow Band at 6.02 GHz	3.58-11.06 GHz UWB with notch at 5.6GHz; narrowband 5.10-5.65 GHz
Gain (dBi)	Not Computed	5dB in the pass band	2dBi in Notched UWB and 3.59dBi in Narrow Band	6dBi in Notched UWB and 3.5dBi in Narrow Band
Component Count	4 Varactor + filter circuit	No active components	2 PIN diodes + SRRs	2 PIN diodes only (reduced complexity)
Complexity	Moderate (multiple components + DGS)	Low (simple layout)	Moderate (SRR placement, dual-mode biasing)	Low-to-Moderate (compact, with simplified biasing)
Configurability Type	Continuous tuning	Fixed notch only	Switchable complementary modes	Switchable complementary modes
Applications	Cognitive radio with SDR (blade RF)	UWB communication, WLAN avoidance	Cognitive radio, MIMO, SDR	Cognitive Radio, IoT, SDR, Dynamic Spectrum Access, Personal Area Networks

The comparison highlights that the proposed FBTA antenna provides frequency-complementary reconfigurable operation, allowing for the use of only two PIN diodes to switch between narrowband and notched UWB modes. The FBTA provides equivalent dual-mode capabilities with fewer elements and a simpler structure than Ref. [3], which utilizes varactor diodes and a more complicated filter design, and Ref. [22], which utilizes PIN diodes along with SRRs. In comparison to Ref. [6], which limits itself to fixed band-notching through passive parasitic elements, the FBTA enables dynamic operation and electrical configurability. In addition, the FBTA supports cognitive radio and SDR applications well and shows better gain performance (6dBi in UWB, 3.5dBi in narrowband). Its compact dimensions and low-to-moderate complexity make it suitable for contemporary wireless systems that require simplicity of integration and efficiency.

## VI. CONCLUSION

A Frequency Band Tunable Antenna (FBTA) is designed and presented in this paper, which has reconfigurable characteristics from notched ultra wideband to narrow band in the WLAN licensed band. Frequency band configurability is implemented by loading the antenna with an open-ended triangular parasitic element and PIN diodes embedded on the ground plane. The FBTA operating band switches from notched UWB to narrow band response on the biasing conditions of the PIN diodes. In one mode of operation, the FBTA shows band-notched characteristics from 5.16 GHz to 5.97 GHz in Ultra Wideband, and in another mode, Narrow band characteristic from 5.10 GHz

to 5.65 GHz. The FBTA antenna can be operated in either Notched UWB or Narrow band mode, which allows the antenna to be a frequency-complementary reconfigurable antenna. The proposed FBTA antenna model is designed and validated by comparing the simulated results with the measured results.

## REFERENCES

- [1] Federal Communications Commission. Revision of part 15 of the commission's rules regarding ultra-wideband transmission systems. FIRST REPORT AND ORDER FCC 02-48, 2002.
- [2] Chang, K., H. Kim, and Y. J. Yoon. "Ultra-wideband antenna with improved gain characteristics." *IET microwaves, antennas & propagation*, vol. 2, no. 5, pp. 512-517, 2008.
- [3] Ibrahim, Ahmed A., et al. "Tunable filtenna with DGS loaded resonators for a cognitive radio system based on an SDR transceiver." *IEEE Access*, vol. 10, pp. 32123-32131, 2022.
- [4] Lai, Hanyu, et al. "UWB antenna with dual band rejection for WLAN/WiMAX bands using CSRRs." *Progress in Electromagnetics Research Letters*, vol. 26, pp. 69-78, 2011.
- [5] Bahadori, Keyvan, and Yahya Rahmat-Samii. "A miniaturized elliptic-card UWB antenna with WLAN band rejection for wireless communications." *IEEE Transactions on Antennas and Propagation*, vol. 55, no. 11, pp. 3326-3332, 2007.
- [6] Kim, K. H., Y. J. Cho, S. H. Hwang, and SeongOok Park. "Band-notched UWB planar monopole antenna with two parasitic patches." *Electronics Letters*, vol. 41, no. 14, p. 1, 2005.
- [7] Ma, Tzyh-Ghuang, Ren-Ching Hua, and Chin-Feng Chou. "Design of a multiresonator loaded band-rejected ultrawideband planar monopole antenna with controllable notched bandwidth." *IEEE Transactions on Antennas and Propagation*, vol. 56, no. 9, pp. 2875-2883, 2008.
- [8] Wu, Sung-Jung, Cheng-Hung Kang, Keng-Hsien Chen, Chao-Kai Chan, and Jenn-Hwan Tarnq. "A notched-band UWB planar monopole antenna using the tapped-line coupled resonator." *In 2009 Asia Pacific Microwave Conference*, pp. 2486-2489. IEEE, 2009.
- [9] Zhu, Jianfeng, et al. "Compact dual-polarized UWB quasi-self-complementary MIMO/diversity antenna with band-rejection capability." *IEEE Antennas and Wireless Propagation Letters*, vol. 15, pp. 905-908, 2015.
- [10] Gheethan, Ahmad A., and Dimitris E. Anagnostou. "Dual band-reject UWB antenna with sharp rejection of narrow and closely-spaced bands." *IEEE transactions on antennas and propagation*, vol. 60, no. 4, pp. 2071-2076, 2012.
- [11] Sohail, Amir, et al. "Dual notch band UWB antenna with improved notch characteristics." *Microwave and Optical Technology Letters*, vol. 60, no. 4, pp. 925-930, 2018.
- [12] Deng, J-Y., Y-Z. Yin, Sh-G. Zhou, and Q-Zh Liu. "Compact ultra-wideband antenna with tri-band notched characteristic." *Electronics Letters*, vol. 44, no. 21, pp. 1231-1233, 2008.
- [13] Chattha, Hassan Tariq, Farah Latif, Farooq A. Tahir, Muhammad Umar Khan, and Xiaodong Yang. "Small-sized UWB MIMO antenna with band rejection capability." *IEEE Access*, vol. 7, pp. 121816-121824, 2019.
- [14] Yang, Hailong, Jinsheng Zhang, Xuping Li, Yapeng Li, Junhua Yang, and Xiaomin Shi. "Design and analysis of UWB antenna with quintuple band-notched and wide-band rejection characteristics." *International Journal of Microwave and Wireless Technologies*, vol. 15, no. 2, pp. 271-281, 2023.
- [15] Modak, Sumon, Surender Daasari, Partha Pratim Shome, and Taimoor Khan. "Switchable/tunable band-notched characteristics in UWB and UWB-MIMO antennas: A comprehensive review." *Wireless Personal Communications*, vol. 128, no. 3, pp. 2131-2154, 2023.
- [16] Ayinala, Kabir Das, and Prasanna Kumar Sahu. "Isolation Enhanced Compact Dual-Mode 4-Port MIMO Design Using Slot-Based Switchable DGS Decoupling Filters." *Wireless Personal Communications*, vol. 135, no. 2, pp. 805-833, 2024.
- [17] Kumar, Gurpreet, Daljeet Singh, and Rajeev Kumar. "A planar CPW-fed UWB antenna with dual rectangular notch band characteristics incorporating U-slot, SRRs, and EBGs." *International Journal of RF and Microwave Computer-Aided Engineering*, vol. 31, no. 7, 2021: e22676.
- [18] Hu, Peng Fei, Yong Mei Pan, and Bin-Jie Hu. "Electrically small, planar, complementary antenna with reconfigurable frequency." *IEEE Transactions on Antennas and Propagation*, vol. 67, no. 8, pp. 5176-5184, 2019.
- [19] Suresh, Ankireddy Chandra, and Thatiparthi Sreenivasulu Reddy. "Experimental Investigation of Novel Frock-Shaped Miniaturized 4x 4 UWB MIMO Antenna Using Characteristic Mode Analysis." *Progress in Electromagnetics Research B*, vol. 101, 2023.
- [20] Shaik, Kareemulla, and Vijay Kumar. "Compact triple band notched UWB MIMO antenna with integrated GSM." *International Journal of Communication Systems*, 2024: e5708.
- [21] Yadav, Dinesh, Mahesh Pandurang Abegaonkar, Shibani K. Koul, Vivekanand N. Tiwari, and Deepak Bhatnagar. "A novel frequency reconfigurable monopole antenna with switchable characteristics between band-notched UWB and WLAN applications." *Progress In Electromagnetics Research C*, vol. 77, pp. 145-153, 2017.
- [22] Saha, Chinmoy, Jawad Y. Siddiqui, Alois P. Freundorfer, Latheef A. Shaik, and Yahia MM Antar. "Active reconfigurable ultra-wideband antenna with complementary frequency notched and narrowband response." *IEEE Access*, vol. 8, pp. 100802-100809, 2020.
- [23] Balanis, Constantine A. *Antenna theory: analysis and design*. John Wiley & sons, 2016.